

Diverting Hydrogenations with Wilkinson's Catalyst towards Highly Reactive Rhodium(I) Species

Jesus E. Perea-Buceta, Israel Fernández, Sami Heikkinen, Kirill Axenov, Alistair W. T. King, Teemu Niemi, Martin Nieger, Markku Leskelä, and Timo Repo*

Abstract: The addition of Barton's base has a dramatic effect on the classic rhodium(III)-mediated hydrogenations promoted by Wilkinson's catalyst. Following the initial oxidative addition, a barrierless reductive elimination of HCl from the traditional rhodium(III) intermediates instantly produces a rhodium(I) monohydride species, which is remarkably reactive in the hydrogenation of several internal alkynes and functionalized trisubstituted alkenes. The direct formation of this species is unprecedented upon addition of molecular hydrogen and its catalytic potential has been hitherto barely explored.

Hydrogen not only finds ordinary use in innumerable chemical transformations,^[1] but is also the simplest model molecule to study low-energy catalytic pathways towards the activation of most inert σ bonds.^[2] The discovery of Wilkinson's catalyst ($[\text{Rh}(\text{PPh}_3)_3\text{Cl}]$; **1**)^[3] was instrumental in the fundamental understanding of metal–H interactions and hydrogen activation.^[4] Subsequently, this landmark has triggered a rapid evolution on the rational design of hydrogenation catalysts,^[5] which in turn, have nurtured a burgeoning progress in other key areas such as asymmetric catalysis,^[6] energy storage, and C–H activation.^[7]

Mechanistically, the catalytic hydrogenation of olefins with **1** is the customary textbook example of a two-electron catalytic redox cycle. First, H_2 adds oxidatively to the rhodium(I) center, thus forming a rhodium(III) dihydride. Comprehensive studies carried out by Halpern proved that the 16-electron complex $[\text{H}_2\text{Rh}(\text{PPh}_3)_2\text{Cl}]$ is the kinetically competent rhodium(III) species to which the olefin then coordinates and undergoes the rate-limiting migratory insertion step.^[8] Finally, reductive elimination generates the hydrogenated product and closes the catalytic cycle.^[9] Conventional NMR techniques only allow the detection of off-cycle species such as $[\text{H}_2\text{Rh}(\text{PPh}_3)_3\text{Cl}]$.^[10] However, these are connected with the transient active rhodium(III) species by

well-known phosphine dissociation/reassociation equilibria.^[11]

Despite counting with this thoroughly studied mechanism, and an outstanding performance as the benchmark catalyst in a number of processes including complex late-stage hydrogenations,^[12] little is known to overcome the well-documented limitations of **1** without previously modifying its inner coordination sphere.^[1,5] In the course of our ongoing efforts on small-molecule activation and bifunctional metal-free hydrogenations,^[13] we became interested in the synergetic catalytic potential of adding an external base to the classic hydrogenation of apolar multiple bonds catalyzed by **1**.

For the study, we bore in mind that the addition of an external base into a metal-based catalytic hydrogenation system usually causes the stepwise deprotonation of a weak $\text{M}-\eta^2\text{-H}_2$ bonded intermediate, or the corresponding dihydride species.^[14] In the case of **1**, several structural factors preclude the stabilization of a $\text{M}-\eta^2\text{-H}_2$ bond, hence a stronger base and drastic reaction conditions would be required to deprotonate the stronger $\text{Rh}-\text{H}$ bonds featured in the resulting neutral dihydride intermediates.^[15]

To begin our research, we conceived that the hydrogenation of a mildly reactive internal alkyne, such as **2a**, would constitute a convenient model system (Table 1). First we examined the effect of the steric hindrance of the external base on the catalytic activity of **1**. Starting with Et_3N , the use of increasingly strained aliphatic tertiary amines, such as **6–8**, or aromatic ones (**9**), had negligible effects upon mild reaction conditions (PhMe, 0.5 bar H_2 , RT). This observation indicated that such tertiary amines just play a spectator role.

We next assessed the impact of adding stronger bases. Polysubstituted guanidines seemed to be obvious candidates given also their tunable sterics.^[16] Whilst TMG (**10**; $\text{p}K_{\text{a}}$ of conjugated acid in MeCN is ca. 23.6) and its proton sponge derivative (**11**; $\text{p}K_{\text{a}} \approx 25.1$) failed to induce any change, a nearly seven-fold boost of catalytic activity was observed with 2-*t*BuTMG (**12**; $\text{p}K_{\text{a}} \approx 26$). Moreover, another base of similar strength to **12**, such as phosphazene (**13**; $\text{p}K_{\text{a}} \approx 28$), promoted a similar increase of activity in relation to the catalyst operating alone.

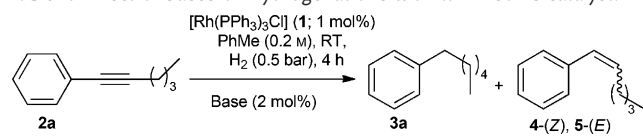
The promising outcome of the initial screening encouraged us to extend the observed catalytic amplification to a series of alkenes and alkynes (Table 2). We commenced by optimizing the reaction conditions for the hydrogenation of **2a** (see Section S11 in the Supporting Information). Raising the reaction concentration (PhMe, 0.5 M) and H_2 pressure (1.0 bar), and the use of **12** (5 mol %), furnished **3a** in an excellent yield of 90% upon isolation. Conversely, similar reaction conditions failed to promote an analogous effect on

[*] Dr. J. E. Perea-Buceta, Dr. S. Heikkinen, Dr. K. Axenov, Dr. A. W. T. King, T. Niemi, Dr. M. Nieger, Prof. M. Leskelä, Prof. T. Repo
Department of Chemistry
P.O.Box 55, 00014 University of Helsinki (Finland)
E-mail: timo.repo@helsinki.fi

Dr. I. Fernández
Departamento de Química Orgánica I, Facultad de Ciencias Químicas, Universidad Complutense de Madrid
Ciudad Universitaria, 28040 Madrid (Spain)

Supporting information for this article is available on the WWW under <http://dx.doi.org/10.1002/anie.201506216>.

Table 1: Effect of bases on hydrogenations with Wilkinson's catalyst.^[a]



Reaction scheme: **2a** (alkyne) + $[Rh(PPh_3)_3Cl]$ (1; 1 mol%), PhMe (0.2 M), RT, H_2 (0.5 bar), 4 h, Base (2 mol%) → **3a** (alkane) + **4a** (alkene, Z/E).

Chemical structures of bases **11**, **12**, and **13** are shown below the reaction scheme.

Entry	Base	Yield [%] ^[b]	3 a	(Z)-4/(E)-5
1	—	12	22:0.3	
2	Et_3N (6)	11	21:0.4	
3	$(iPr)(tBu)NMe$ (7)	13	22:0.3	
4	TMP (8)	14	23:0.5	
5	Ph-TMP (9)	13	22:0.3	
6	TMG (10)	2	10:0.2	
7	11	15	19:0.5	
8	12	69	12:1.2	
9	13	73	12:1.6	

[a] **2a** (1 equiv), **1** (0.01 equiv), base (**6–13**; 0.02 equiv), PhMe (0.2 M), H_2 (0.5 bar), RT, 4 h. [b] Yields determined by GC-MS analysis with mesitylene as an internal standard. For full details, see the Supporting Information. TMP = 2,2,6,6-tetramethylpiperidine, TMG = tetramethylguanidine.

the hydrogenation of **2a** with **1** operating alone, in accord with the classic mechanism where changes in the pressure of H_2 have no effect on the rate-limiting step.^[8] This result indicates that the addition of **12** promotes a mechanistic switch manifested by the key role that the activation of H_2 acquires in the overall reaction kinetic profile. Even more drastic differences between the classical and new basic reaction conditions were observed during the hydrogenation of internal alkynes such as **2b** and **2c**. Whilst **2b** could be fully converted into **3b** under the new base-enhanced reaction conditions, no reactivity was noticed in the absence of **12**.

Remarkably, the alkynylaniline **2c** was also only completely hydrogenated under basic conditions (2 mol% of **1**, 10 mol% of **12**, 1.5 bar H_2) to furnish **3c** in 90% yield after 16 hours (Table 2). No signs of the cycloisomerization reactions, which this family of substrates typically undergoes with a broad variety of metals including rhodium(I), were detected.^[17] Unfortunately, this functional-group tolerance was not observed in terminal alkynes featuring acidic hydrogen atoms as the alkyne **2d** was only converted into the corresponding alkane **3d** under classical reaction conditions. However, negligible catalytic amplification was observed for challenging hindered alkenes such as limonene and α -pinene. To our surprise, this detrimental effect of an increased level of olefin substitution did not appear during the hydrogenation under

basic conditions of the benchmark substrate **2g**.^[18] Indeed, a boost of yield from 27 to 90% was afforded by merely adding 5 mol% of **12**.

A similar trend was observed in going from 2-cyclohexenone (**2e**) to the methyl-substituted analogue **2f**. Whilst a severe decrease on the catalytic activity occurred on classical hydrogenation conditions (**3e**: 84% and **3f**: 13%), the addition of **12** (5 mol%) maintained high product yields (**3e**: 87% and **3f**: 79%) by just elevating the H_2 pressure from 0.5 to 1.5 bar, and expanding the reaction time from 8 to 24 hours (Table 2).

The catalytic amplification was also remarkable with a relatively complex substrate, such as (5*R*)-(–)-carvone (**2h**), containing two different double bonds and a chiral center. In practice, the addition of **12** (10 mol%) to a reaction mixture with **1** (2 mol%) under 1.5 bar of H_2 , raised the isolated yield of the desired hydrogenated product **3h** from 3 to 61%.

We then sought to elucidate, through NMR spectroscopy, the origin of the reactivity promoted by the addition of **12**. In line with the catalytic screening, addition of an excess (4 equiv) of a hindered tertiary amine such as PhTMP failed to promote any changes either in the 1H and $^{31}P\{^1H\}$ NMR spectra of **1** (see Sections S1 and S2), or $[H_2Rh(PPh_3)_3Cl]$ (**14**; Figure 1a,b).^[11]

Identical NMR profiles also arose after adding 4 equivalents of **12** to **1** under Ar (see Section S3), thus indicating no interaction between the base and the rhodium center prior to exposure to H_2 . However, an immediate change of color from orange to yellow announced rapid reaction (ca. 5–10 s at RT) after charging 1.0 bar of H_2 into this mixture. Indeed, a new scenario emerged in the 1H NMR spectrum with a broad signal at $\delta = 10.68$ ppm, characteristic of a guanidinium cation $N-H$, and a $Rh-H$ region only featuring a broad singlet at $\delta = -8.26$ ppm (Figure 1c). Moreover, this species (**15**) undergoes fast intra/intermolecular ligand exchange equilibria in solution at room temperature.^[19]

We next undertook further spectroscopic studies at low temperature to study the fluxional regime of **15** and gain

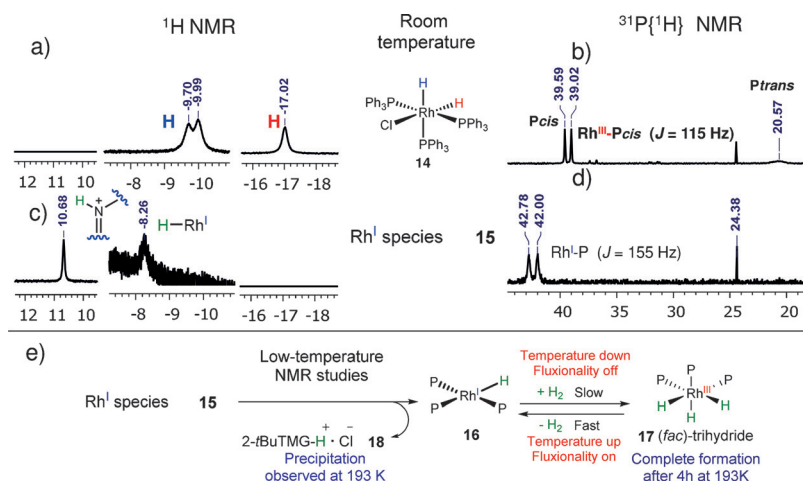
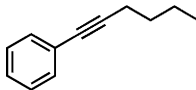
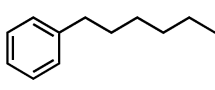
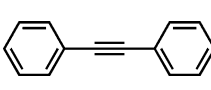
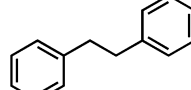
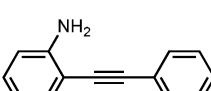
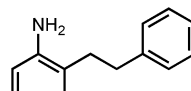
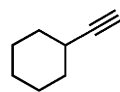
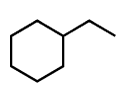
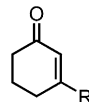
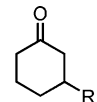
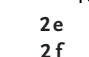
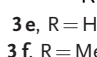
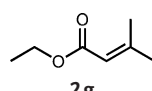
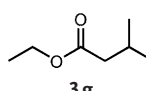
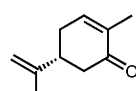
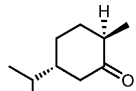


Figure 1. Diagnostic areas in the 1H and $^{31}P\{^1H\}$ NMR spectra (RT, $[D_3]THF$, 1.0 bar of H_2) of **14** (a,b), **15** (c,d), and species observed in the low and variable NMR studies (e). For further details, see the Supporting Information and DFT calculations. For clarity the PPh_3 ligands are labeled P.

Table 2: Impact of the base **12** on the hydrogenations with **1**.^[a]

Substrate	Major product	Cat. (mol %)	P(H ₂) [bar]	t [h]	Yield [%] ^[b] no base 12	
 2a	 3a	1	1.0	4	16	97(90)
 2b	 3b	1	1.0	6	1	99(96)
 2c	 3c	2	1.5	16	0	96(90) ^[c,d]
 2d	 3d	1	1.0	3	98	7 ^[e]
 2e	 3e , R = H	1	0.5	8	84	87 ^[f]
 2f	 3f , R = Me	1	1.5	24	13	79
 2g	 3g	1	1.5	8	27	90
 2h	 3h	2	1.5	20	3	76(61) ^[d,g]

[a] Unless stated otherwise: **2a–h** (1 equiv), **12** (0.05 equiv), PhMe (0.5 M), RT. [b] Yields determined by GC-MS analysis with mesitylene as an internal standard. Yields of the isolated products are given within parentheses. [c] Reaction with **12** (0.1 equiv) and PhMe (0.25 M). [d] Yield determined by ¹H NMR spectroscopy using mesitylene as an internal standard. [e] No alkane detected. Listed yield corresponds to the alkene. [f] Reaction with PhMe (0.2 M) at 0.5 bar of H₂. [g] Reaction with **12** (0.1 equiv). **3h** was isolated in 91–94% purity. (For full details, see Section S12 in the Supporting Information.)

further insight into the mechanism. Upon cooling the mixture to 193 K, the ¹H, ¹H{³¹P}, and ³¹P{¹H} NMR spectra showed that **15** evolved into two other complexes, **16** and **17** (Figure 1 e; see Section S5). The species **16** can be assigned as [Rh(PPh₃)₃H] which was first reported by Shriver et al.^[20] This species results from the dehydrochlorination of the rhodium(III) species **14** promoted by **12** in the presence of H₂. This assignment was fully confirmed by ¹H–³¹P and ³¹P–³¹P two-dimensional correlation NMR measurements (see Section S5). Eventually, a white precipitate was extensively deposited on the NMR tube, which was later identified as the hydrochloride salt of 2-*t*-BuTMG (**18**; see Figure S6.3). This was an unexpected result since **16** is only known to be

prepared by treating **1** with either an equimolar amount of lithium dimethylamide and an excess of dimethylamine,^[20] or with an excess of Et₃SiH,^[21] but not directly in the presence of molecular H₂.

The complex **17** is produced by the reaction of H₂ with **16** at low temperature and was identified as (*fac*)-[Rh(PPh₃)₃(H)₃] (Figure 1 e).^[22] Furthermore, we observed the gradual conversion of rhodium(I) complex **16** into rhodium(III) complex **17** by maintaining the mixture at 193 K (completion after 4–6 h; see Figure S6.2). At such temperatures the mixture is in a nearly-zero fluxional regime and thus there is no steric barrier preventing free H₂ from approaching and reacting with the rhodium(I) center.

To confirm the feasibility of the dehydrochlorination event and also preclude alternative heterolytic pathways compatible with the origin of the observed rhodium(I) species, the rhodium(III) complex **14** was preformed instantaneously under H₂ and the resulting solution was frozen (Figure 2). The H₂ atmosphere was replaced by Ar to avoid equilibration with **1**, and an excess of **12** was added. To our delight, we observed how the Rh^{III}–H resonances of **14** gradually disappeared while the Rh^I–H resonances slowly emerged.^[23] Repetition of the experiment demonstrated that the rate of the process varied with the rate of H₂ diffusion in the NMR tube (see Section S8). Therefore, our experimental findings indicate a detour in the classical hydrogenation mechanism promoted by **1**, which involves the formation of a rhodium(I) species by reaction of the rhodium(III) dihydride complex **14** with **12**.

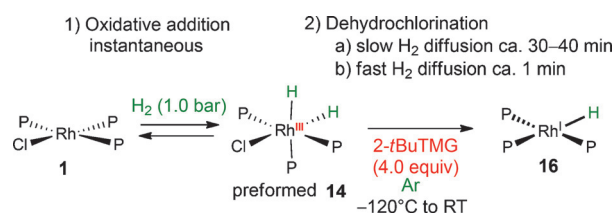


Figure 2. Control NMR studies. The PPh₃ groups are labeled P (for full details see the Supporting Information).

In addition, the ^1H NMR spectra of **15** and $[\text{Rh}(\text{PPh}_3)_3\text{H}]$ (**16**) are quite similar, thus indicating that both species are strongly related. However, there is a noticeable difference, namely a slight broadening and shifting of the Rh–H resonance in **15** (see Figure S9.4).^[24] This change may be ascribed to the occurrence of a weak interaction between the hydride and the guanidine proton, an interaction which is known to provoke a similar effect in related organometallic systems.^[25] Indeed, we found that when a pure sample of $[\text{Rh}(\text{PPh}_3)_3\text{H}]$ is treated with 4 equivalents of $[\text{H}-t\text{BuTMG}][\text{PF}_6]$, a similar broadening of the Rh–H resonance is observed. Furthermore, the corresponding T_1 relaxation time of $\text{Rh}^{\text{I}}\text{–H}$ measured at 300 K decreases from 0.89 to 0.80 seconds (see Section S9), and is fully compatible with the occurrence of such weak H \cdots H interaction.

To gain more insight into the nature of **15**, we carried out a DFT study (see Section S14). Our calculations indicate that indeed a weak Rh–H \cdots HN interaction exists in **15** (Figure 3).

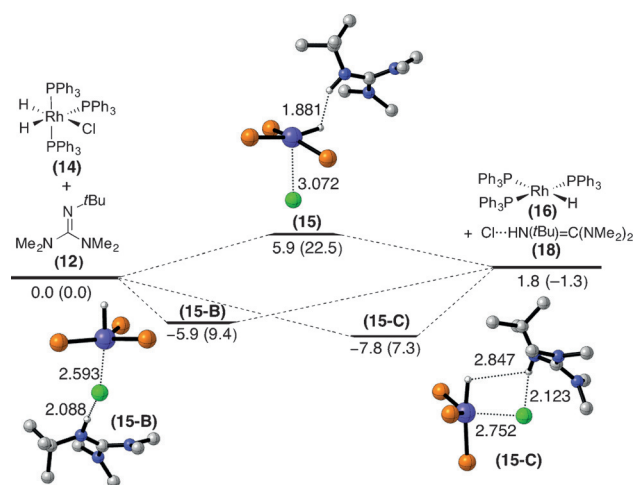


Figure 3. Reaction profile calculated [PCM(toluene)-M06/def2-SVP//M06/def2-SVP level] for the formation of **15** from **14** and **12**. Bond distances and relative electronic energies (ZPVE included) and free energies (within parentheses) are given in Å and kcal mol^{-1} , respectively. The Ph rings in the PPh_3 ligands are omitted for clarity.

The corresponding computed H \cdots H distance of 1.881 Å concurs quite well with that computed for related dihydrogen-bonded iridium complexes.^[25] Despite that, the formation of **15** from **14** and **12** seems unlikely in view of the endergonicity computed for this reaction.^[26] This discovery suggests that the broadening of the $\text{Rh}^{\text{I}}\text{–H}$ resonance may be caused by a different weak interaction occurring in $[\text{Rh}(\text{PPh}_3)_3\text{H}]$.^[27] Indeed, two different species, **15B** and **15C**, were located on the potential energy surface and they lie 11.8 and 13.7 kcal mol^{-1} , respectively, below the dihydrogen-bonded species **15** (Figure 3). In these complexes, the weak interaction is established between the transition metal and the Cl of the protonated guanidine (computed Rh \cdots Cl distance of 2.593 and 2.752 Å, respectively). Further experimental support for this Rh \cdots Cl intermolecular interaction is given by the ^1H NMR spectrum of a mixture of pure $[\text{Rh}(\text{PPh}_3)_3\text{H}]$ with

4 equivalents of $[\text{NBu}_4]\text{Cl}$, a solution which also exhibits a similar broadening of the Rh–H signal (corresponding T_1 value of 0.92 s; see Section S9).

Finally, we were interested in understanding the key dehydrochlorination event. Unfortunately, all our attempts to locate a transition state for the direct conversion of **14** into **15** on the potential energy surface met with no success. This outcome is very likely because of the steric hindrance in **14** preventing the approach of the bulky base **12**. Hence, it can be suggested that a PPh_3 ligand dissociation occurs first in the Rh^{III} complex **14** (leading to complex $[\text{H}_2\text{Rh}(\text{PPh}_3)_2\text{Cl}]$, **19**) to facilitate the reaction with **12**. Strikingly, relaxed scans performed at different Rh \cdots H distances starting from **19** (where Rh–H = 1.6 Å, that is, a similar bond length in complex **14**) nicely show that the abstraction of the hydride promoted by **12** is essentially a barrierless process (see Figure S14.1).

Furthermore, our calculations also suggest that this process is assisted by the chloride ligand, which starts to dissociate during the transformation (i.e. the Rh–Cl bond becomes longer and longer as the H abstraction takes place). As a result, the initial Rh–Cl bond in **1** can easily dissociate, thus forming $[\text{Rh}(\text{PPh}_3)_3\text{H}]$ (**16**) and the hydrochloride salt **18**, as experimentally observed. Therefore, the diversion in the classical hydrogenation mechanism can be formally viewed as a barrierless reductive elimination of HCl from rhodium(III) species **14** as a result of H abstraction by **12**, thus ultimately giving **15**, a complex similar to $[\text{Rh}(\text{PPh}_3)_3\text{H}]$.

In conclusion, we have discovered an unprecedented, facile, and efficient manner to amplify the reactivity of the benchmark catalyst **1** in situ without modifying its inner coordination sphere. The simple addition of a strong base (**12**) in catalytic amounts gives rise to highly reactive rhodium(I) species for the hydrogenation of a series of alkynes and functionalized trisubstituted alkenes. Extensive spectroscopic NMR analyses combined with DFT studies identified a barrierless reductive elimination of HCl, promoted by **12**, from the classic dihydride rhodium(III) species **14** as the key event leading to the observed catalytic scenario. Ongoing studies are pursued in our laboratories to further explore prospective catalytic applications for this type of reactivity.

Acknowledgements

The work was supported by the Academy of Finland (139550, 276586) and the Spanish MINECO-FEDER (grant CTQ2013-44303-P).

Keywords: density functional calculations · homogeneous hydrogenation · reaction mechanisms · rhodium(I) · Wilkinson's catalyst

How to cite: *Angew. Chem. Int. Ed.* **2015**, *54*, 14321–14325
Angew. Chem. **2015**, *127*, 14529–14533

[1] *Handbook of Homogeneous Hydrogenation* (Eds.: J. G. de Vries, C. J. Elsevier), Wiley-VCH, Weinheim, **2007**.

- [2] a) F. Maseras, A. Lledós, E. Clot, O. Eisenstein, *Chem. Rev.* **2000**, *100*, 601–636; b) G. J. Kubas, *Proc. Natl. Acad. Sci. USA* **2007**, *104*, 6901–6907.
- [3] a) J. F. Young, J. A. Osborn, F. H. Jardine, G. Wilkinson, *Chem. Commun.* **1965**, 131–132; b) J. A. Osborn, F. H. Jardine, J. F. Young, G. Wilkinson, *J. Chem. Soc. A* **1966**, 1711–1732; c) J. Halpern, C. S. Wong, *J. Chem. Soc. Chem. Commun.* **1973**, 629–630.
- [4] a) P. G. Jessop, R. H. Morris, *Coord. Chem. Rev.* **1992**, *121*, 155–284; b) M. Torrent, M. Solá, G. Frenking, *Chem. Rev.* **2000**, *100*, 439–493; c) G. J. Kubas in *Metal Dihydrogen and σ -Bond Complexes* (Ed.: J. P. Fackler Jr.), Kluwer, New York, **2002**, pp. 259–295.
- [5] J. F. Hartwig in *Organotransition metal chemistry-From Bonding to Catalysis* (Ed.: J. F. Hartwig), University Science Books, Mill Valley, U.S., **2010**, pp. 575–667.
- [6] R. Noyori, *Angew. Chem. Int. Ed.* **2013**, *52*, 79–92; *Angew. Chem.* **2013**, *125*, 83–98.
- [7] W. D. Jones, in *Comprehensive Organometallic Chemistry III, Vol. 1*, (Ed.: G. Parkin), Elsevier Science, Amsterdam, **2007**, pp. 699–723.
- [8] J. Halpern, *Inorg. Chim. Acta* **1981**, *50*, 11–19.
- [9] a) A. Dedieu, *Inorg. Chem.* **1980**, *19*, 375–383; b) C. Daniel, N. Koga, J. Han, X. Y. Fu, K. Morokuma, *J. Am. Chem. Soc.* **1988**, *110*, 3773–3787; c) T. Matsubara, R. Takahashi, S. Asai, *Bull. Chem. Soc. Jpn.* **2013**, *86*, 243–254.
- [10] S. B. Duckett, C. L. Newell, R. Eisenberg, *J. Am. Chem. Soc.* **1994**, *116*, 10548–10556.
- [11] a) P. Meakin, J. P. Jesson, C. A. Tolman, *J. Am. Chem. Soc.* **1972**, *94*, 3240–3242; b) C. A. Tolman, P. Z. Meakin, D. I. Lindner, J. P. Jesson, *J. Am. Chem. Soc.* **1974**, *96*, 2762–2774.
- [12] a) N. Waizumi, A. R. Stankovic, V. H. Rawal, *J. Am. Chem. Soc.* **2003**, *125*, 13022–13023; b) A. Fürstner, T. Nagano, *J. Am. Chem. Soc.* **2007**, *129*, 1906–1907.
- [13] a) V. Sumerin, F. Schulz, M. Nieger, M. Leskelä, T. Repo, B. Rieger, *Angew. Chem. Int. Ed.* **2008**, *47*, 6001–6003; *Angew. Chem.* **2008**, *120*, 6090–6092; b) V. Sumerin, F. Schulz, M. Atsumi, C. Wang, M. Nieger, M. Leskelä, T. Repo, P. Pyykkö, B. Rieger, *J. Am. Chem. Soc.* **2008**, *130*, 14117–14119; c) K. Chernichenko, A. Madarász, I. Pápai, M. Nieger, M. Leskelä, T. Repo, *Nat. Chem.* **2013**, *5*, 718–723; d) T. Niemi, J. E. Perea-Buceta, I. Fernández, S. Alakurtti, E. Rantala, T. Repo, *Chem. Eur. J.* **2014**, *20*, 8867–8871; e) M. Lindqvist, K. Borre, K. Axenov, B. Kótai, M. Nieger, M. Leskelä, I. Pápai, T. Repo, *J. Am. Chem. Soc.* **2015**, *137*, 4038–4041.
- [14] a) M. G. Basallote, M. Besora, E. Castillo, M. J. Fernández-Trujillo, A. Lledós, F. Maseras, M. A. Mániz, *J. Am. Chem. Soc.* **2007**, *129*, 6608–6618; b) Y.-Y. Jiang, H.-Z. Yu, Y. Fu, *Organometallics* **2014**, *33*, 6577–6584; c) R. R. Schrock, J. A. Osborn, *J. Am. Chem. Soc.* **1976**, *98*, 2143–2147.
- [15] a) M. Tilset in *Comprehensive Organometallic Chemistry III, Vol. 1* (Ed.: G. Parkin), Elsevier Science, Amsterdam, **2007**, pp. 279–305; b) J. R. Norton in *Organotransition metal chemistry-From Bonding to Catalysis* (Ed.: J. F. Hartwig), University Science Books, Mill Valley, U.S., **2010**, pp. 129–146.
- [16] D. Margetic, in *Superbases for Organic Synthesis* (Ed.: T. Ishikawa), Wiley, Hoboken, **2009**, pp. 9–48.
- [17] B. M. Trost, A. McClory, *Angew. Chem. Int. Ed.* **2007**, *46*, 2074–2077; *Angew. Chem.* **2007**, *119*, 2120–2123.
- [18] R. P. Yu, J. M. Darmon, C. Milsmann, G. W. Margulieux, S. C. E. Stieber, S. DeBeer, P. J. Chirik, *J. Am. Chem. Soc.* **2013**, *135*, 13168–13184.
- [19] J. Goodman, V. V. Grushin, R. B. Larichev, S. A. Macgregor, W. J. Marshall, D. C. Roe, *J. Am. Chem. Soc.* **2010**, *132*, 12013–12026.
- [20] a) S. H. Strauss, S. E. Diamond, F. Mares, D. F. Shriver, *Inorg. Chem.* **1978**, *17*, 3064–3068; b) S. H. Strauss, D. F. Shriver, *Inorg. Chem.* **1978**, *17*, 3069–3074.
- [21] M. A. Esteruelas, J. Herrero, M. Oliván, *Organometallics* **2004**, *23*, 3891–3897.
- [22] Validation of this assignment was provided by extensive spectroscopic analysis (see Section S5), and a close fit with the data reported for the analogous (*fac*)-[Rh(PEt₃)₃(H)₃]: T. Braun, D. Noveski, M. Ahijado, F. Wehmeier, *Dalton Trans.* **2007**, 3820–3825.
- [23] [H₂Rh(PPh₃)₃Cl] was observed by NMR in the reaction mixture of **1**, **12** (4 equiv), and H₂ (1.0 bar) 30 s after melting the sample at 173 K. The rhodium(I) monohydride species was observed after 1 min (see Section S8).
- [24] The difference between the identity of the rhodium(I) species **15** and [Rh(PPh₃)₃H] was underlined by their respective catalytic activities in the hydrogenation of 2-alkynylaniline (**2c**; see Section S13), and their different Rh^I–H signals (see Section S9).
- [25] See, for instance: A. Rossin, E. I. Gutsul, N. V. Belkova, L. M. Epstein, L. Gonsalvi, A. Lledós, K. A. Lyssenko, M. Peruzzini, E. S. Shubina, F. Zanolini, *Inorg. Chem.* **2010**, *49*, 4343–4354.
- [26] We also computed the formation of the corresponding dihydrogen-bonded cation where the chloride ligand is already dissociated. The **14** + **12** → [(Ph₃P)₃RhH⁺⋯H(*t*Bu)N=C(NMe₂)₂]⁺ + Cl[−] process is even more unlikely ($\Delta E = +47.1$ kcal mol^{−1}, $\Delta G = +55.7$ kcal mol^{−1}).
- [27] A reviewer suggested that the broadening of the Rh–H resonance might be related with a dynamic equilibrium between [Rh(PPh₃)₃H] and small amounts of cluster species in solution, as it was proposed before: A. J. Sivak, E. L. Muetterties, *J. Am. Chem. Soc.* **1979**, *101*, 4878–4887.

Received: July 6, 2015

Revised: August 5, 2015

Published online: October 6, 2015